

# Phase Behavior and Mechanical Properties of Blends of Poly(butylene terephthalate) and Poly(amino-ether) Resin

A. Granado, J. I. Eguiazábal, J. Nazábal

*Departamento de Ciencia y Tecnología de Polímeros and Instituto de Materiales Poliméricos "POLYMAT," Facultad de Ciencias Químicas UPV/EHU, P. O. Box 1072, 20080 San Sebastian, Spain*

Received 8 January 2003; accepted 12 May 2003

**ABSTRACT:** The structure, thermal and mechanical properties of blends of poly(butylene terephthalate) (PBT) and a poly(amino-ether) (PAE) barrier resin obtained by direct injection molding are reported. The slight shift of the glass transition temperatures ( $T_g$ ) of the pure components when blended is attributed to partial miscibility rather than interchange reactions. Both the small strain and the break properties of the blends were close or even above those predicted by the direct rule of mixtures. The specific volume of the

blends appeared to be the main reason for the modulus behavior. The linear values of the elongation at break indicated that the blends were compatible, and were attributed to a combination of good adhesion between the two phases of the blends and the small size of the dispersed phases. © 2003 Wiley Periodicals, Inc. *J Appl Polym Sci* 91: 132–139, 2004

**Key words:** blends; phase behavior; mechanical properties

## INTRODUCTION

Polymer blends are one of the most investigated fields in polymer science and technology.<sup>1</sup> This is because they offer a fast and cheap way to obtain new polymeric materials with a combination of properties often difficult to find in a single polymer.<sup>1–3</sup> Among polymer blends, those of condensation polymers, such as polyesters, polyamides and polycarbonates, have been widely investigated.<sup>1,4–8</sup> This is due both to their favorable combination of properties, their high potential for specific interactions between their phases, and their common tendency to react during processing to produce copolymers. These last two characteristics tend to make the interphase adhesion large enough to compatibilize the blends.<sup>9–11</sup>

Poly(butylene terephthalate) (PBT) is a semicrystalline engineering polyester with many positive performance characteristics, such as high heat and solvent resistance, remarkable strength and toughness, and low viscosity in the melt state.<sup>12</sup> Poly(amino-ether) (PAE) resins are thermoplastic amorphous materials that have recently been commercialized. They are generally obtained by the condensation reaction of diglycidyl ethers with a variety of amines,<sup>13</sup> giving rise to different chemical structures. PAE resins show high gas barrier protection, good adhesion to a variety of substrates, mechanical toughness, high optical quality and low color. These properties make PAE resins suit-

able for new barrier packaging applications, and potentially suitable for replacing glass and metal in containers.

Many PBT based blends have been studied. Among them, miscible blends with phenoxy,<sup>14,15</sup> poly(ethylene terephthalate),<sup>16</sup> polyarylate,<sup>17</sup> poly(ester-carbonate)<sup>18</sup> and polycarbonate<sup>19</sup> have been studied. Partially miscible blends have been obtained with polycarbonate,<sup>4,20</sup> poly(ester-carbonate),<sup>18</sup> and liquid-crystal polymers (LCP's).<sup>7,21</sup> Polyamide 66,<sup>22</sup> polyamide 6<sup>23,24</sup> and linear low density polyethylene,<sup>25,26</sup> for instance, form immiscible blends. Reactions have been seen, for example, in blends with polyarylate,<sup>17</sup> phenoxy,<sup>27</sup> polycarbonate<sup>28</sup> and poly(ester-carbonate).<sup>29</sup> However, to our knowledge no study has been published on blends with PAE resins.

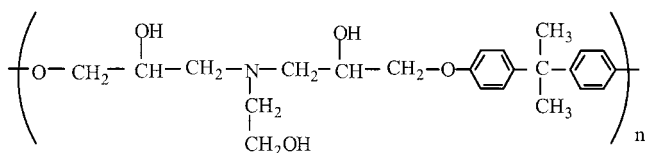
Thus, the combination of the properties of PBT and PAE appears to be promising, but the phase behavior and mechanical properties of the blends have not been studied. In this work, we studied the miscibility and mechanical properties of blends of PBT with a PAE resin across the whole composition range. The blends were obtained by direct injection molding. The phase structure of the blends was characterized by differential scanning calorimetry (DSC), dynamic mechanical analysis (DMA) and Vicat softening temperature measurements. The morphology was analyzed by scanning electron microscopy (SEM), and the mechanical properties were determined by tensile tests.

## EXPERIMENTAL

The polymers used in this work were PBT (Crastin PBT, Du Pont, Mechelen, Belgium) and a PAE resin

Correspondence to: J. I. Eguiazábal (popهوري@sq.ehu.es).

kindly supplied by Dow Chemical (Midland, MI) under the trade name Blox. The PAE is the product of the polycondensation of the diglycidyl ether of bisphenol A and ethanolamine and has the following chemical structure:



Both polymers were dried before processing, PBT for 8 h at 110°C and PAE for 6 h at 65°C. The PBT/PAE blends were directly melt mixed and injection molded over a range of compositions using a Battenfeld BA230E reciprocating screw injection molding machine at a melt temperature of 230°C and a mold temperature of 15°C. The screw had a diameter of 17.8 mm and a L/D ratio of 17.8. No mixing devices were present. Tensile (ASTM D-638 type IV) specimens were obtained.

To check for the possible development of inter-change reactions during melt mixing, the torque of mixing, which is related to the melt viscosity, was measured in a Brabender batch kneader at 230°C and 30 rpm as a function of residence time.

The phase behavior of the blends was studied by DSC and DMA. The DSC scans were carried out using a Perkin-Elmer DSC-7 calorimeter at a heating rate of 20°C/min in a nitrogen atmosphere. Two heating scans were carried out between 10 and 250°C. Cooling between both scans was carried out at the maximum rate provided by the calorimeter. The glass transition and melting temperatures, and the melting enthalpies, were determined in the second scan. The crystallinity of PBT was calculated from the melting enthalpies of the blends and the melting enthalpy of the 100% crystalline PBT ( $\Delta H_m^0 = 145.5$  J/g).<sup>5</sup> DMA tests were carried out in a Polymer Laboratories apparatus, at a frequency of 1 Hz in the flexural mode and at a heating rate of 4°C/min from -100°C to 130°C. The  $T_g$  values were determined as the maximum of the tan  $\delta$ -temperature plots. Vicat softening temperatures were determined according to ASTM D1525 (50°C/h and 1000 g).

The tensile tests were carried out in an Instron 4301 tester at a crosshead speed of 10 mm/min. The mechanical properties, Young's modulus ( $E$ ), yield stress ( $\sigma_y$ ), and break strain ( $\epsilon_b$ ), were determined from the force-displacement curves. A minimum of eight specimens was tested for each reported value.

Quantitative measurements of the orientation were obtained by attenuated total reflectance (ATR) infrared spectroscopy.<sup>30-35</sup> The polarized ATR spectra were carried out at a 45° angle of incidence using a Nicolet Magna-IR 560 spectrophotometer equipped with an ATR accessory (Spectra-Tech). The resolution

was 8 cm<sup>-1</sup>, and three measurements were carried out for each reported value. The dichroic ratio,  $D$ , was the ratio of the intensities of the absorption band of a characteristic group measured for parallel ( $A_{\parallel}$ ) and perpendicular ( $A_{\perp}$ ) polarization with respect to the injection direction,

$$D = \frac{A_{\parallel}}{A_{\perp}}$$

The carboxyl vibration, from 1743 to 1678 cm<sup>-1</sup>, was used to investigate PBT orientation. However, the analysis of PAE and the blends was carried out using the absorption band located between 1053 and 999 cm<sup>-1</sup>. The average orientation was expressed as the orientation function ( $f$ ) that is related to the dichroic ratio as

$$f = \frac{(D - 1)(D_0 + 2)}{(D + 2)(D_0 - 1)}$$

where  $D_0 = 2 \cot^2 \alpha$ , and  $\alpha$  is the angle between the chain axis and the transition moment. Although  $\alpha$  is not accurately known, 90° can be used as a first approximation for all perpendicular bands, because this angle would give rise to the minimum orientation value.

Density measurements were carried out on a Mirage SD-120L electronic densitometer, using *n*-butyl alcohol as the immersion liquid. The temperature was controlled with a precision of  $\pm 0.1^\circ\text{C}$ . The specific volume of the amorphous phase was obtained from the experimental density values using the equation:

$$\frac{1}{\rho_b} = \frac{1 - X_{\text{PBTc}}}{\rho_a} + \frac{X_{\text{PBTc}}}{\rho_{\text{PBTc}}}$$

where  $X_{\text{PBTc}}$  is the crystalline content of the blend calculated by DSC as described previously,  $\rho_a$  is the experimental density of the amorphous phase of the blend and  $\rho_{\text{PBTc}}$  is the density of crystalline PBT (1.396 g/cm<sup>3</sup>).<sup>4</sup>

The surfaces of both the tensile (at room temperature) and the cryogenically fractured specimens were observed by SEM (Hitachi S-2700) after gold coating (Jeol JFC 1100 fine coat ion sputter) and at an accelerating voltage of 15 kV. Cryogenic fracture was carried out after immersing the specimens for 75 min in liquid nitrogen (-196°C). The cryogenically fractured surfaces of the PBT-rich and intermediate blends were immersed in tetrahydrofuran (THF) for 210 min to dissolve the PAE phase. Then they were cleaned with the same solvent and left to dry in air.

## RESULTS AND DISCUSSION

### Torque behavior

As is known, the melt viscosity, and consequently the torque of kneading, usually change when the chemical

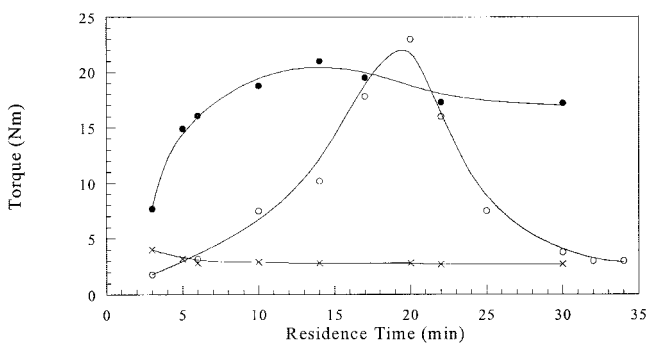


**Figure 1** Torque values versus residence time for (×) PBT, (○) PAE, (●) 50/50 blend.

nature of melt blends changes through chemical reactions.<sup>24,36–38</sup> If reactions do not take place, then after melting the torque remains constant with kneading time, or, in the case of degradation, it decreases slightly. PAE has three lateral hydroxyl groups in its repeat unit, which are probably able to react with the carboxyl groups of PBT. This kind of reaction has previously been seen in blends of PBT with phenoxy,<sup>14,36</sup> which also has a lateral hydroxyl group. Therefore, provided that the blending time is long enough, interchange reactions leading to grafted or crosslinked products will probably occur in PBT–PAE blends.

The torque profiles taken in a batch kneader for PBT, PAE, and the 50/50 PBT–PAE blend are shown in Figure 1. As can be seen, the torque of PBT remained practically constant with residence time, indicating that no appreciable degradation took place under the kneading conditions used. However, in the case of both the neat PAE and the PBT–PAE 50/50 blend, the torque increased to a maximum value, after which it decreased. The behavior of PAE is unusual for a pure polymer, but, as mentioned above, it has lateral hydroxyl groups that may react. This must be the source of the torque increase. In the case of the 50/50 blend, the torque increase took place after a short blending time. This torque increase cannot be due to reactions among PAE molecules because they need a longer time to react. Therefore, it indicates a reaction between the two components of the blend. The reaction was probably an alcoholysis reaction between PAE hydroxyl groups and PBT carboxyl groups.<sup>7</sup> Similar results were obtained by Robeson and coworkers<sup>14</sup> and by Nazabal and coworkers<sup>36</sup> for the PBT–phenoxy system, and also by Nazabal and coworkers<sup>6</sup> for phenoxy–PC blends, and were attributed to the formation of grafted or crosslinked copolymers.

As can also be seen in Figure 1, in the case of pure PAE after the maximum torque value, there was a strong decrease, and a nonfusible powder product was obtained. However, in the 50/50 blend, the torque

decrease after the maximum was less pronounced, and the final product was a viscous melt able to flow with no presence of powder at all. This indicates that the fast alcoholysis reactions between PBT and PAE did not allow reaction between PAE molecules to take place, and thus crosslinking occurred to a very low extent, if at all.

### Phase behavior

The  $T_g$  values of the injection molded blends, determined by DSC, are plotted against blend composition in Figure 2. As can be seen, two  $T_g$  values were observed for the blends with 10 and 20% PAE. One  $T_g$  value was slightly below that of pure PAE, and the other was above that of PBT. The low temperature  $T_g$  could not be properly observed in PAE-rich and intermediate compositions. This was due to its small intensity, which was probably a consequence of the high crystallinity of PBT, which will be discussed below. The shift of each  $T_g$  value toward that of the other component indicates the presence of two phases in the PBT-rich blends, each of them containing minority amounts of the other component.

To fully study the phase behavior of the blends, they were also tested by DMA, which usually provides a detection level higher than that of DSC. Figure 3(a) shows  $\tan \delta$  as a function of temperature for both the two pure components and some of the blends. As can be seen, the  $T_g$  of PAE was approximately 80°C, while that of PBT was approximately 60°C. The sharp  $T_g$  peak of PAE contrasts the broad, less defined peak of PBT. All of the blends showed a clear  $T_g$  slightly below that of PAE. The  $T_g$  decrease was greater as the PBT content in the blends increased. No peak could be observed near 60°C, but the presence of a shoulder in all blends was very clear. The position of the peak represented by the shoulder cannot be determined accurately, due to its breadth. Figure 3(b) shows the storage modulus ( $E'$ ) as a function of temperature. As can be seen, the intensity of the glass transition of PBT

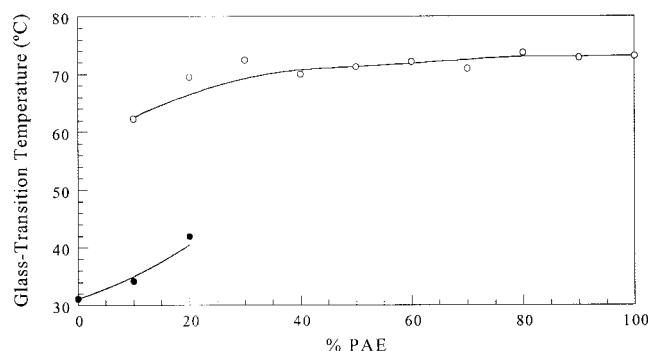


**Figure 2**  $T_g$  versus composition of PBT–PAE blends, determined by DSC.

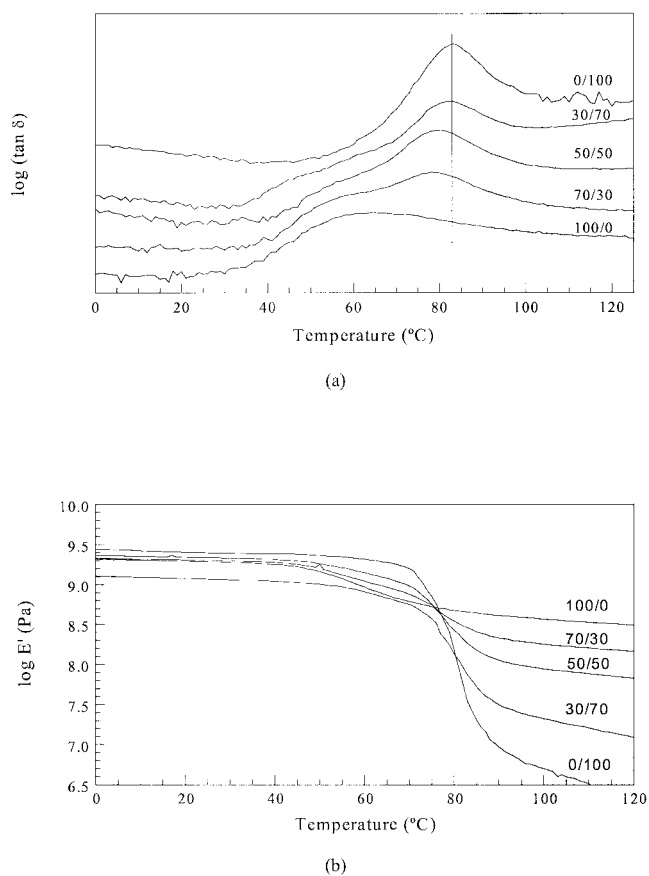


**Figure 3** DMA of PBT-PAE blends versus temperature: (a)  $\log(\tan \delta)$  and (b)  $\log(E')$ .

is much smaller than that of PAE. As a consequence, in the blends, the  $E'$  drop that corresponds to the  $T_g$  of the PAE-rich phase is clearly displayed, but the value that corresponds to the  $T_g$  of the PBT-rich phase is difficult to observe. This is due to the wide temperature range at which it appears.

The observed  $T_g$  shifts in the blends could be due to either partial miscibility or the development of interchange reactions during processing. The estimated residence time of the blends in the injection machine was approximately 2.5 min, so that, according to Figure 1, the reaction level of the blends in the solid state should be low. The possibility of reaction was also studied by FTIR, comparing the FTIR spectra of the blends with the theoretical spectra obtained by weighted addition of the spectra of the components. The experimental and theoretical spectra were very similar, indicating that the reaction level in the blends was negligible. Consequently, the presence of the minority component in each phase of the blends is attributed to partial miscibility.

The approximate compositions of the two amorphous phases of the blends can be estimated from the experimental  $T_g$  values and the Fox equation:<sup>39</sup>

$$\frac{1}{T_g} = \frac{w_1}{T_{g1}} + \frac{w_2}{T_{g2}}$$

where  $T_g$  is the glass transition temperature of the blend obtained by DSC,  $T_{g1}$  and  $T_{g2}$  are the glass transition temperatures of pure PBT and PAE respectively and  $w_1$  and  $w_2$ , their corresponding weight fractions in each amorphous phase. As can be seen in Table I, the maximum calculated PBT content in the PAE-rich phase was 24%, and was found for the PBT-PAE 90/10 blend. In the rest of the blends, the variations observed were mostly negligible, as the observed  $T_g$  shifts were similar to the estimated error of the measurement. The 80/20 blend had a PAE content in the amorphous PBT-rich phase of 29%. It also had both the maximum PAE content and an observable PBT-rich amorphous phase  $T_g$ . It is probable that the blends with high PAE content have an even higher PAE presence in the PBT-rich phase. Thus, the maximum miscibility of PAE in the PBT-rich phase will be above 29%, and PAE is more miscible in PBT than PBT is in PAE.

No cold crystallization exothermic peaks appeared in the DSC scans, indicating that PBT was fully crystallized. This was in spite of the rapid cooling that takes place in both the injection mold and the calorimeter, and indicates that PAE practically did not hinder PBT crystallization. This behavior was similar to that reported by Nazabal and coworkers for both PBT-PEC<sup>29</sup> and polyamide 6-phenoxy<sup>9</sup> systems. The melting temperature ( $T_m$ ) values of PBT were practically constant (226 °C) with composition, in spite of the partial miscibility of the blends. This indicated that the presence of PAE did not affect the perfection of the PBT crystallites. This is an usual behavior in immiscible and partially miscible systems<sup>22,29</sup> that is also seen in miscible blends.<sup>40</sup>

The crystalline content of PBT was determined by DSC. The crystallinity of pure PBT (30%) was retained in the blends, indicating both that the PAE presence had practically no effect on PBT crystallization and

**TABLE I**  
Minor Component Weight Fraction in the Two Amorphous Phases of PBT-PAE Blends

PBT/PAE	PBT-Rich Phase (%)	PAE-Rich Phase (%)
90/10	9	24
80/20	29	8
70/30	—	2
60/40	—	6
50/50	—	4
40/60	—	2
30/70	—	4
20/80	—	1
10/90	—	2

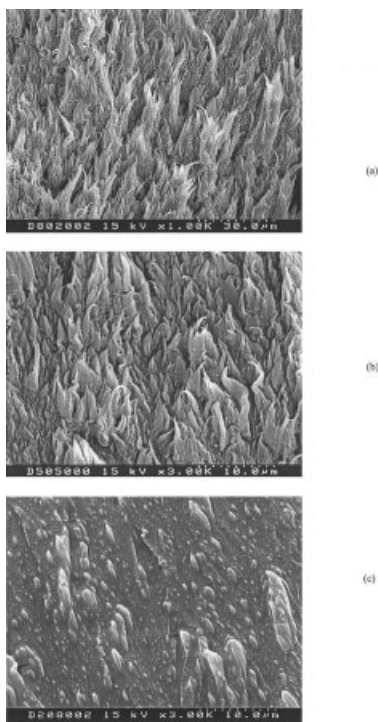


**Figure 4** Surfaces of tensile fractured specimens: (a) 80/20, (b) 50/50 and (c) 20/80 compositions.

that PBT crystallized even when mixed in the PAE-rich phase.

### Morphology

The tensile fractured surfaces of the 80/20, 50/50 and 20/80 compositions are shown respectively in Figures 4(a, b and c). The surfaces of the other PBT-rich blends were similar to that of Figure 4(a), and those of PAE-rich blends were similar to that of Figure 4(c). In PBT-rich blends, a highly fibrillated PBT morphology perpendicular to the fracture surface appeared. Similar morphologies were obtained for both PBT-polycarbonate<sup>4</sup> and polyamide 6-phenoxy<sup>9</sup> blends. In Figure 4(c), only slightly elongated PBT particles were seen, probably due to the comparatively low ductility of the PAE matrix. Adhesion appeared to be good, as shown in Figure 4(c), because no voids surrounding the dispersed phase were seen.

To better observe both the interphase and the morphology of the blends, the cryogenic fracture surfaces were observed by SEM. In PBT-rich and intermediate compositions, the two phases of the blends could not be discerned, indicating both cohesive fracture and high interfacial adhesion. The morphology of the 20/80 composition is shown in Figure 5. The morphology was fairly homogeneous, and the dispersed phase size was small (typically  $0.3\ \mu\text{m}$ ). Moreover, adhesion was high, as no voids were seen around the dispersed particles.

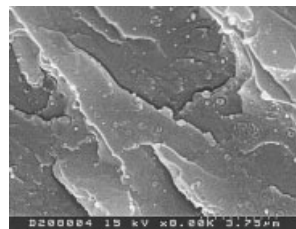


**Figure 5** Cryogenically fractured surface of a PBT-PAE 20/80 specimen.

To observe the morphology of the PBT-rich and intermediate compositions, the cryogenically fractured surfaces were treated with THF. The surfaces of the 70/30 and 50/50 compositions are shown respectively in Figures 6(a, b). The dispersed phase appeared to be distributed homogeneously, and the particle size was small, with most particles below  $0.6$  and  $1\ \mu\text{m}$  respectively in the 70/30 and 50/50 blends. The fraction of voids was smaller than expected from the blend composition, probably due to the large presence of PAE in the PBT-rich phase.

It is known that the Vicat test provides information about the phase behavior of polymer blends,<sup>41</sup> so that the phase inversion composition of biphasic blends can be deduced from the Vicat softening temperature-composition plots. The results for PBT-PAE blends are plotted in Figure 7. The Vicat temperature of the blends was similar to that of PBT up to the 60/40 composition, and similar to that of PAE beyond the 40/60 blend, indicating the presence of the respective matrices. The Vicat temperature of the 50/50 blend was clearly closer to that of PBT-rich blends, indicating the presence of a PBT-rich matrix. This agrees with

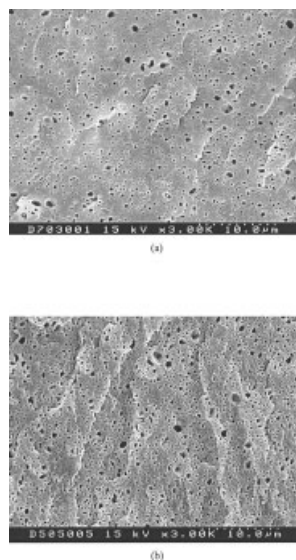


**Figure 6** Surfaces of cryogenically fractured specimens treated with THF: (a) 70/30 and (b) 50/50 compositions.

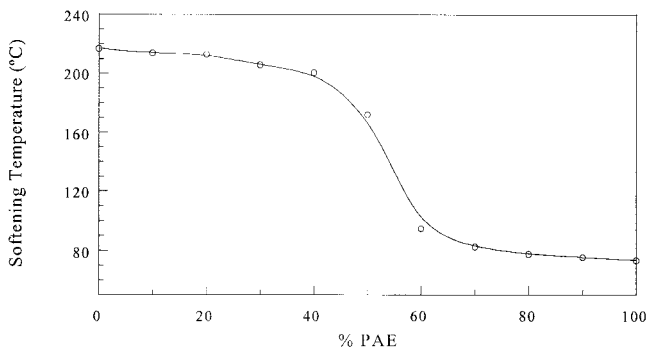


Figure 7 Vicat softening temperature of blends versus composition.

the morphology observed in Figure 6(b). The inflexion point took place between the 50/50 and 40/60 compositions, where the phase inversion should be located.

**Mechanical properties**

The Young's moduli of the blends are plotted against composition in Figure 8. The plot is very close to the values predicted by the linear rule of mixtures (linear reference line), and, with the exception of the 90/10 blend, the moduli were slightly below linearity. This modulus behavior could be due to (i) a different crystallinity of PBT in the blends and in the neat state, (ii) a different orientation in the blends and in the pure components, or (iii) an increase in free volume of the components upon blending. The crystalline content of PBT measured in the first scan did not change with composition. Therefore, a PBT crystallinity change with the blend composition was not the reason for the modulus behavior.

The orientation of the blend components both in the pure state and in blends rich in each of the two components was studied by infrared spectroscopy.<sup>30,31</sup> PBT was not oriented ( $f = 0$ ), and PAE showed some orientation ( $f = 0.16$ ), which was further proved by its

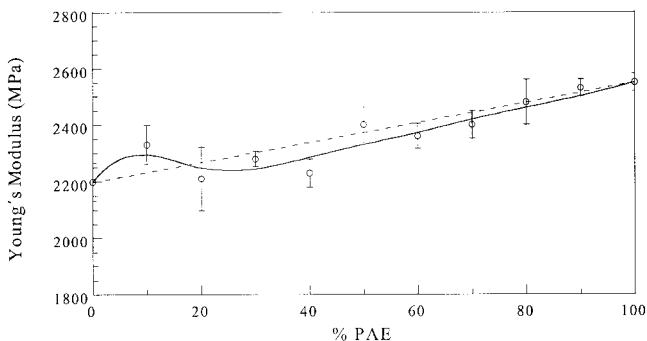


Figure 8 Young's modulus of the blends versus composition.

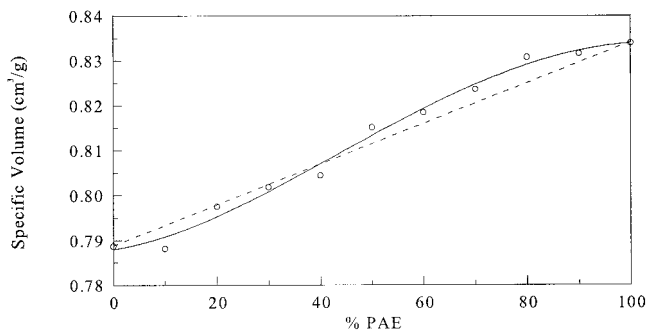


Figure 9 Specific volume of the amorphous part of the blends versus composition.

observed shrinkage on annealing (8%). Although this shrinkage could not be measured in neat PBT due to crystallization, the blends with 10, 20 and 70% PAE showed  $f$  values that corresponded to the proportions of the two pure components. This linear change of the orientation of the blends with composition indicates that a different orientation in the blends was not the reason for the observed deviations in the modulus of elasticity.

In Figure 9, the specific volume of the amorphous part of the blends is shown against composition. Comparing Figures 8 and 9, the shapes of both plots are clearly related. This is because most of the blends showed a positive deviation from the rule of mixtures in the specific volume, which agreed with the negative deviations of the modulus. Moreover, in the case of the 90/10 blend, the opposite took place. Thus, the change in specific volume of the amorphous part of the blends appears to be the main factor that determines the modulus of elasticity of the blends.

The yield stresses of the blends against composition are shown in Figure 10. The yield stress of the 90/10 blend showed the largest positive deviation from the rule of mixtures, in agreement with both the modulus and the specific volume values. However, the values of the other compositions are less clearly related to the plots of Figures 8 and 9, as a slight positive yield stress

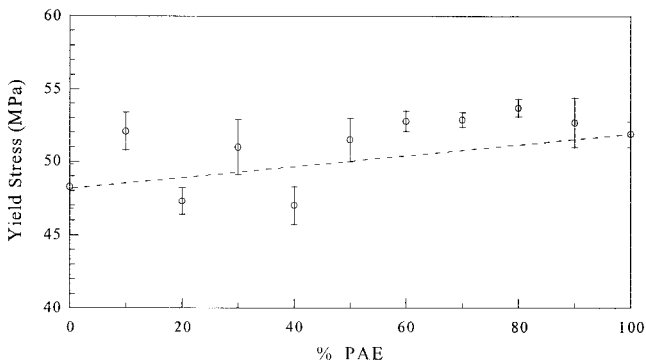
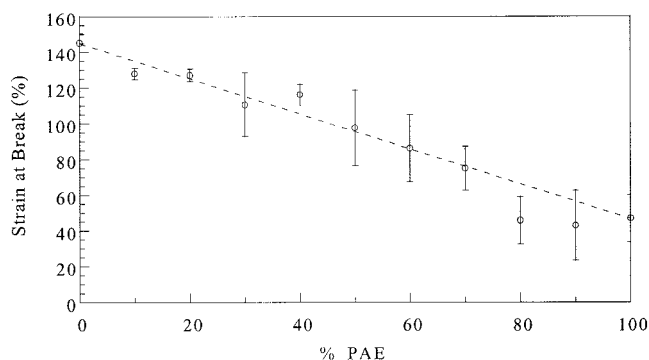


Figure 10 Yield stress of the blends versus composition.



**Figure 11** Strain at break of the blends versus composition.

deviation appeared. The behaviors of both the Young's modulus and yield stress are usually similar, but differences have also been observed.<sup>42</sup>

The plot of ductility against composition is shown in Figure 11. The values are adequately described by the simple rule of mixtures. It is known that a small dispersed phase size is necessary to obtain compatible polymer blends<sup>26,37,42</sup> This is because the large stress concentrations provoked by large dispersed particles lead to early failure. The low dispersed phase size of PBT-PAE blends (0.4-1  $\mu\text{m}$ ) is probably one reason for the observed positive behavior, which has also been seen in partially miscible blends such as polyetherimide-polyarylate<sup>43</sup> It is also known that, although significant exceptions exist,<sup>44</sup> the strain at break usually depends strongly on the blend miscibility,<sup>26,45</sup> and more specifically on the interfacial adhesion between components.<sup>1</sup> The almost linear behavior of ductility with composition displayed in Figure 11 indicates that, as was seen previously from the morphological observations, the adhesion between the blend components was good enough to allow an efficient stress transfer from the matrix to the dispersed phase.<sup>9,38,46</sup> This positive response of a break property such as ductility shows the compatible nature of these blends.

## CONCLUSIONS

Directly injection molded PBT-PAE blends are composed of two amorphous phases, each rich in one of the two components. The presence of minor amounts of the other component in each amorphous phase was detected by the change in  $T_g$  values of the components in the blends and was attributed to partial miscibility rather than to reactions. The change of the specific volume is proposed as the main parameter that determines the behavior of the Young's modulus, rather than changes in orientation or crystallinity upon blending. The linearity, or slight synergism observed in ductility, is attributed to the small size of the dis-

persed phase, and indicates both good interfacial adhesion and compatibility of the blends.

The financial support of the University of the Basque Country (Project no. 203.215-13540/2001) is gratefully acknowledged. The authors also acknowledge Dr. Ha Q. Pham and Dr. Asjad Shafi, from Dow Chemical, for supplying the PAE sample. A. Granado acknowledges the Basque Government for the award of a grant for the development of this work.

## References

- Paul, D. R.; Bucknall, C. B. *Polymer Blends*; Academic Press: New York, 2000.
- Utracki, L. A. In *Polymer Alloys and Blends*; Hanser: New York, 1990; Chapter 1.
- Paul, D. R. In *Polymer Blends*; Paul, D. R., Newman, S., Eds.; Academic Press: New York, 1978; Chapter 1.
- Sánchez, P.; Remiro, P. M.; Nazábal, J. *J Appl Polym Sci* 1993, 50, 995.
- Vallejo, F. J.; Eguiazábal, J. I.; Nazábal, J. *J Appl Polym Sci* 2001, 80, 885.
- Mondragón, I.; Gaztelumendi, M.; Nazábal, J. *Polym Eng Sci* 1986, 26, 1478.
- Porter, R. S.; Wang, L.-H. *Polymer* 1992, 33, 2019.
- Kotliar, A. M. *J Polym Sci: Macromol Rev* 1981, 16, 367.
- Guerrica-Echeverría, G.; Eguiazábal, J. I.; Nazábal, J. *J Appl Polym Sci* 1999, 72, 1113.
- Fried, J. R.; Hanna, G. A. *Polym Eng Sci* 1982, 22, 705.
- Kleiner, L. W.; Karasz, F. E.; MacKnight, W. J. *Polym Eng Sci* 1979, 19, 519.
- Brydson, J. A. *Plastic Materials*; Butterworth-Heinemann: Oxford, 1999.
- Silvis, H. C.; White, J. E. *Polym News* 1998, 23, 6.
- Robeson, L. M.; Furtek, A. B. *J Appl Polym Sci* 1979, 23, 645.
- Martínez, J. M.; Eguiazábal, J. I.; Nazábal, J. *J Macromol Sci-Phys* 1991, 30, 345.
- Avramova, N. *Polymer* 1995, 36, 801.
- Kimura, M.; Porter, R. S.; Salee, G. *J Polym Sci Part B: Polym Phys* 1983, 21, 367.
- Rodríguez, J. L.; Eguiazábal, J. I.; Nazábal, J. *J Macromol Sci-Phys* 1997, 36, 773.
- Mishra, S. P.; Venkidasamy, P. *J Appl Polym Sci* 1995, 58, 2229.
- Reekmans, B. J.; Nakayama, K. *J Appl Polym Sci* 1996, 62, 247.
- Qi, K.; Nakayama, K. *J Mater Sci* 2001, 36, 3207.
- Huang, C.-C.; Chang, F.-C. *Polymer* 1997, 38, 2135.
- An, J.; Ge, J.; Liu, Y. *J Appl Polym Sci* 1996, 60, 1803.
- Chiou, K.-C.; Chang, F.-C. *J Polym Sci Part B: Polym Phys* 2000, 38, 23.
- Kang, T.-K.; Kim, Y.; Lee, W.-K.; Park, H.-D.; Cho, W.-J.; Ha, C.-S. *J Appl Polym Sci* 1999, 72, 989.
- Yang, J.; Shi, D.; Yao, Z.; Xin, Z.; Yin, J. *J Appl Polym Sci* 2002, 84, 1059.
- Eguiazábal, J. I.; Cortázar, M.; Iruin, J. J.; Guzmán, G. M. *J Macromol Sci-Phys* 1988, 27, 19.
- Devaux, J.; Godard, P.; Mercier, J. P. *Polym Eng Sci* 1982, 22, 229.
- Rodríguez, J. L.; Eguiazábal, J. I.; Nazábal, J. *Polym J* 1996, 28, 501.
- Ward, I. M. *Structure and Properties of Oriented Polymers*; Applied Science: London, 1975.
- Noda, I.; Dowrey, A. E.; Marcott, C. In *Fourier Transform Infrared Characterization of Polymers*; Ishida, H., Ed.; Plenum Press: New York, 1987.
- Bensaad, S.; Jasse, B.; Noel, C. *Polymer* 1999, 40, 7295.

33. Pirnia, A.; Sung, C. S. P. *Macromolecules* 1988, 21, 2699.
34. Schmidt, P.; Kolarik, J.; Lednický, F.; Dybal, J.; Lagarón, J. M.; Pastor, J. M. *Polymer* 2000, 41, 4267.
35. Aji, A.; Guèvremont, J.; Cole, K. C.; Dumoulin, M. M. *Polymer* 1996, 37, 3707.
36. Eguiazábal, J. I.; Nazábal, J. *J Mater Sci* 1990, 25, 1522.
37. Zhang, H. X.; Hourston, D. J. *J Appl Polym Sci* 1999, 71, 2049.
38. Locke, C. E.; Paul, D. R. *J Appl Polym Sci* 1973, 17, 2597.
39. Fox, T. G. *Bull Am Phys Soc* 1956, 1, 123.
40. Eguiazábal, J. I.; Iruin, J. J. *Mater Chem Phys* 1987, 18, 147.
41. Bastida, S.; Eguiazábal, J. I.; Nazábal, J. *Polym Test* 1993, 12, 233.
42. Bastida, S.; Eguiazábal, J. I.; Nazábal, J. *Polymer* 1996, 37, 2317.
43. Bastida, S.; Eguiazábal, J. I.; Nazábal, J. *Eur Polym J* 1996, 32, 1229.
44. Arzak, A.; Eguiazábal, J. I.; Nazábal, J. *Macromol Chem Phys* 1997, 198, 1829.
45. Samios, C. K.; Kalfoglou, N. K. *Polymer* 2000, 41, 5759.
46. James, S. G.; Donald, A. M.; Miles, I. S.; Mallagh, L.; MacDonald, W. A.; *J Polym Sci: Polym Phys* 1993, 31, 221.